Euro. Jnl of Applied Mathematics (2001), *vol.* 12, *pp.* 367–393. Printed in the United Kingdom

Droplet profiles under the influence of van der Waals forces

ELIJAHU MINKOV[1] and AMY NOVICK-COHEN[2]

[1]*Department of Computer Science, Technion–IIT, Haifa 32000, Israel*
[2]*Department of Mathematics, Technion–IIT, Haifa 32000, Israel*

(*Received 25 October 1999; revised 20 December 2000*)

We study the effect of van der Waals forces on globally energy minimizing profiles for liquid droplets which lie on a solid substrate in a vapour atmosphere and which are assumed to have a uniform cross-section. We prove that for repulsive van der Waals forces as well as for certain short range repulsive-long range attractive forces, there exists a unique globally minimizing profile. Although this profile necessarily contains vertical bounding segments, the height A of the vertical bounding segments can often be demonstrated to be order of magnitude smaller that the overall height B of the droplet. This is the case, in particular, when the droplet is sufficiently large, the Hamaker constant is sufficiently small, and the attractive forces are sufficiently mild. In the presence of repulsive forces only, A is on the order of angströms when B is on the order of millimeters, for realistic parameter values. Moreover, conditions are prescribed under which Young's law is satisfied to leading order despite the appearance of the vertical segments, when the contact angle is measured via an inscribed circle construction at a distance ξ_0 from the edge of the droplet, where $A \ll \xi_0 \ll B$.

1 Introduction

It has been classically conjectured that if the profile $\xi(x, y)$ of a droplet lying on a substrate in a vapour atmosphere is assumed to be single-valued, then the sessile droplet form can be predicted by minimizing the energy

$$F[\xi] = \int_\Omega [-S + \gamma(1 + \xi_x^2 + \xi_y^2)^{\frac{1}{2}} + G(\xi)]\, dx\, dy \tag{1.1}$$

where ξ is constrained to belong to a suitable class of functions. Here Ω denotes the wetted region, which is to be determined up to translation by the minimization process. The first term in (1.1) represents the wetting energy, and S, the spreading coefficient, is given by $S = \gamma_{SV} - \gamma_{SL}$, where γ_{SV} and γ_{SL} are respectively the interfacial energies per unit area of the solid-vapour and solid-liquid interfaces. The second term represents the surface energy of the bounding droplet-vapour surface, and γ is the interfacial energy per unit area of the liquid-vapour interface. The third term $G(\xi)$ contains the energetic contributions of gravity ($G(\xi) = \int_0^\xi \rho g z\, dz$). Energy minimization of (1.1) must be undertaken in conjunction with a mass constraint

$$M[\xi] = \int_\Omega \rho\xi\, dx\, dy = M_0, \tag{1.2}$$

https://doi.org/10.1017/S0956792501004478 Published online by Cambridge University Press

where ρ is the fluid density, unless the system is taken to be in (thermodynamic) equilibrium with a bulk fluid bath. In that case there is no need to impose a mass constraint, though $G(\xi)$ must then be amplified to include hydrostatic effects. The energy minimization problem (1.1)-(1.2) has been studied in depth (for example, see the book of Finn [7]). The energy minimizing droplet profile must satisfy Laplace's equation as dictated by the Euler–Lagrange necessary condition:

$$2\gamma H(\xi) = \lambda + G'(\xi) \tag{1.3}$$

where $H(\xi)$ denotes the mean curvature and λ is a Lagrange multiplier, and the droplet must contact the solid substrate in such a manner that β, the contact angle, i.e. the angle between the droplet and the substrate, satisfies Young's law:

$$\cos\beta = S/\gamma. \tag{1.4}$$

For simplicity let us assume, as we do throughout this paper, that the droplet profile has a uniform cross-section, i.e. $\xi(x, y)$ is independent of y. In this case Ω can be taken to be one-dimensional, and F and M should be interpreted as the free energy per unit length and the mass per unit length respectively. To gain intuition into the implications of (1.3), we note that (1.3) can be solved explicitely to yield $\xi = \beta x + \mathcal{O}(x^2)$ for the droplet profile of a droplet lying to the right of the point $x = 0$.

The classical formulation fails to take into account the energetic contributions arising from van der Waals forces which become important in close proximity to the contact line of the droplet with the solid surface. These are long range microscopic forces, and their inclusion within the context of a continuum theory is often somewhat problematic. Attempts to generalize the classical formulation in order to take into account these forces has lead to consideration of an "enhanced" free energy

$$F[\xi] = \int_\Omega [-S + \gamma(1 + \xi_x^2 + \xi_y^2)^{\frac{1}{2}} + G(\xi) + P(\xi)]\, dx\, dy, \tag{1.5}$$

where $P(\xi) = -\int_\xi^\infty \Pi(z)\, dz$, where Π is the 'disjoining pressure', has been added to incorporate the effects of van der Waals forces. In the simplest modelling, one may assume that $P(\xi) = \hat{A}\xi^{-\alpha}$, where typically $2 \leqslant \alpha \leqslant 3$. Here $\hat{A}$, the Hamaker constant, may be either positive (reflecting repulsive forces between the droplet surface and the substrate) or negative (reflecting attractive forces between the droplet surface and the substrate). Again, the minimization must be undertaken within a suitable class of functions and in conjunction with a mass constraint.

Under closer examination, it becomes clear that sufficiently close to the point of contact of the droplet with the underlying substrate in the range of several hundreds of angströms, 100–1000 Å, a variety of types of forces can come into play. Such forces can include attractive as well as repulsive van der Waals intermolecular forces, effects of excess interfacial surface charge, and electrical double layers. See the discussion in Oron *et al.* [22]. It has been suggested (Teletzke *et al.* [25]) that these effects could be incorporated into a generalized disjoining pressure. Among the forms of generalized disjoining pressure considered recently are: (i) $\Pi(\xi) = a_3\xi^{-3} - a_9\xi^{-9}$, $a_3, a_9 > 0$, which results from a 6–12 Lennard-Jones potential [15, 16], (ii) $\Pi(\xi) = -a_3\,\xi^{-3} + l_1 \exp(-\xi/l_2)$, $a_3, l_1, l_2 > 0$, which combines repulsive dispersive forces and polar attractive forces [11, 24], and (iii)

https://doi.org/10.1017/S0956792501004478 Published online by Cambridge University Press

$\Pi(\xi) = a_3\xi^{-3} - a_4\xi^{-4}$, with $a_3, a_4 > 0$ which models attractive-repulsive forces in the context of liquid films on solid surfaces coated by corrosive products [21]. Note that sufficiently close to the contact point, the repulsive forces dominate in (i)–(iii). We will refer to attractive-repulsive forces as limiting attractive if $\lim_{\xi\to 0} P(\xi) = -\infty$ and limiting repulsive if $\lim_{\xi\to 0} P(\xi) = \infty$.

To understand the implications of this assortment of generalised disjoining pressures for droplet profiles, in particular, for droplet profiles with uniform cross-section, let us consider the predicted behavior in the vicinity of the contact point. Suppose that an augmented version of (1.3), i.e.

$$2\gamma H(\xi) = \lambda + G'(\xi) + P'(\xi) \tag{1.6}$$

applies in this neighborhood. This would appear to be a reasonable assumption since (1.6) is indeed the Euler–Lagrange equation associated with (1.5) which is applicable if the solution has some minimal regularity in this neighborhood (ξ is absolutely continuous and ξ_x is essentially bounded). Clearly, if $P(\xi)$ is singular at $\xi = 0$, then

$$2\gamma H(\xi) \approx P'(\xi),$$

which has the first integral

$$-2\gamma(1 + \xi_x^2)^{-\frac{1}{2}} \approx P(\xi) + \text{constant}. \tag{1.7}$$

Note that now the boundary condition $\xi_x(0) = \beta$ implied by Youngs law (1.4) cannot be applied in any reasonable fashion if β is finite. For the limiting repulsive forces as well as for the limiting attractive forces, the left hand side of (1.7) remains bounded whereas the right hand side diverges as $x \to 0$. In short, in both cases, the augmented Euler–Lagrange equation (1.6) cannot be valid down to the contact point. The problem then arises as to how to include disjoining (or generalized disjoining) forces and still obtain a reliable prediction of the contact angle. Though much attention has been given to this problem, many open question remain [17], and experimental verification is limited by the use of low resolution microscopy in the context of liquid–fluid–solid contacts, as well as by other more inherent difficulties.

In the present paper we focus on the case of limiting repulsive forces. Since repulsive forces are known to stabilize thin films, as opposed to attractive forces which are known to lead to rupture, this would seemingly be the less problematic case. Within a suitable mathematical framework, we demonstrate the existence of a unique energy minimizing droplet profile which is also physically reasonable. More specifically, we define a class of energy densities (see Hypothesis HI) which permits inclusion of a term such as $P(\xi) = \hat{A}\xi^{-\alpha}$, $\hat{A} > 0$ reflecting a simple repulsive disjoining pressure, as well as attractive-repulsive disjoining pressures such as those given in (i)–(iii) if the attractive contributions are suitably restricted. For this class of energy densities we study the energy minimizing droplet profiles. Despite the fact that the Euler–Lagrange equation does not hold – and, as can easily be checked, no solution of the form $\xi(x) \approx sx^a$ can describe the behavior of the droplet profile near the contact point, we prove that a physically viable interpretation of the energy minimization problem can be attained by allowing the droplet profile not to be single-valued – in particular by allowing the droplet profile to contain vertical segments of a suitably small height. Physically, such vertical segments are innocuous if their height

is comparable to that of a molecular layer or two, and contact angle measurements should not be influenced by their existence. Mathematically, such a description can be shown to follow from a suitable parametric formulation of the energy minimization problem coupled together with an 'overtaking strategy'. The feasibility of this approach was already broached in two previous papers [18, 19]. In particular, existence of an energy minimizing profile in this framework was proven in Novick-Cohen [19]. In the present paper we prove the uniqueness of such an energy minimizing profile and obtain a clear characterization of its features. Indeed, we show that under suitable additional assumptions, which hold in particular if the droplet is not too small, the Hamaker (or the 'effective' Hamaker) constant is not too large, and the attractive forces are nonsingular and sufficiently mild, Young's contact angle prediction is well approximated by the energy minimizing profile when it evaluated via curvature measurements made at a suitable distance, not too far and not too near, the droplet edge. These assumptions, which can be satisfied by an energy density incorporating a simple repulsive potential as well as a potential of type (ii) under certain restriction on the defining parameters, also guarantee that the relative height of the vertical segments to the overall droplet height is small. Thus, in the context of the present description, Young's law can be said to be lost in the prediction of the sub-microscopic (intrinsic) contact angle, but reappears in the prediction an effective (and measureable) contact angle. The present paper demonstrates that alternate approaches such as regularizing the singular forces by imposing an arbitrary cut-off is really not at all essential; the singular formulation is indeed reasonable and self-consistent.

Preliminary investigations indicate that the problem of determining droplet profiles in the presence of long range repulsive-short range attractive forces should also be amenable to the general methodology of Novick-Cohen [18, 19]. However, in the case of limiting attractive forces, the minimization process leads to droplets which appear to 'float above' or to be minimally attached to the underlying substrate, hence the analysis presented here must be significantly altered to treat this case. Nevertheless, it should still be possible to prescribe a similar type of contact angle measurement at an appropriate distance from the droplet (overhang) edge, which should reproduce classical contact angle predictions under suitable assumptions. We defer further discussion of this case to a later publication.

So far our discussion has been static. Obviously, it would be desirable to be able to view the energy minimizing profile as a steady state attainable as $t \to \infty$ in some appropriate dynamical setting, i.e. as part of a global attractor. One would hope that a thin film type equation:

$$\mu\xi_t - \tfrac{1}{3}[\xi^3(G'(\xi) + P'(\xi))_x]_x + \frac{\gamma}{3}\left[\xi^3\left[\frac{\xi_{xx}}{(1+\xi_x^2)^{3/2}}\right]_x\right]_x = 0 \tag{1.8}$$

with $\mu > 0$, which reduces to the regular thin film equation

$$\mu\xi_t - \tfrac{1}{3}[\xi^3(G'(\xi) + P'(\xi))\xi_x]_x + \frac{\gamma}{3}(\xi^3\xi_{xxx})_x = 0 \tag{1.9}$$

when $\xi_x^2 \ll 1$, would provide a reasonable framework within which to consider the dynamics. This is not such a readily achieved goal. Even though considerable analytic work has appeared on the thin film and thin film type equations since the publication of the influential work of Bernis & Friedman [1], the equation remains problematic from the theoretical point of view, in particular with regard to the case of nonzero contact

angles. Nevertheless, numerical analysis has been undertaken for (1.9) for disjoining pressures represented in (i)–(iii) [15, 16, 11, 24, 21, 20, 9]. In particular, in Mitlin [15] for potentials of the form *ii*), thick films were seen to rupture and thinner films broke up into droplets separated by ultrathin flat films. Film break up was similarly seen in Grün [9] for disjoining pressures of type *i*) using a nonnegativity preserving numerical scheme. In Oron & Bankoff [21], the difficulties of the thin film equation were avoided by calculating the steady states for an attractive-repulsive potential of type *iii*) within the context of an Allen–Cahn type equation instead of the thin film equation on a periodic domain, where off-hand the set of equilibria should be the same. There, however, contact angles, spreading coefficients and contact line notions were neglected. The results given in Mitlin [15], Oron & Bankoff [21], Oron [20] and Grün [9] are not in contradiction to the results obtained here when one takes into account that (a) the two equations (1.8) and (1.9) differ when ξ_x^2 is not small – and this is an effect which it seems should be noticeable near the contact angle, and (b) in their analysis the profiles have been constrained to be single-valued and Neumann and no-flux or periodic boundary conditions were used. In Oron [20], three-dimensional numerics were undertaken for the thin film equation using a disjoining pressure of type (iii) and periodic boundary conditions. Interesting enough the film evolved to an isolated steady drop standing on a practically flat film. Our analysis, in contrast, is heavily focused on droplets with compact support; thus in seeking an appropriate dynamical setting we must be more careful. So far the only proof of existence for a thin film type equation with a non-zero contact angle has appeared in Otto [23] for the lubrication approximation equation using the relatively recent notion of gradient flow for a prescribed energy with respect to the Wasserstein metric. There, though, disjoining pressure effects were neglected. It is quite conceivable, though not immediately evident, that such a framework would allow a description of droplet dynamics based on an energy of the form (1.5) under suitable assumptions. This framework has also been useful in connecting Hele-Shaw flow with nonzero contact angle with the lubrication approximation [8].

We remark, in passing, that the approach of introducing a cut-off leads to the nonsingular evolution equation

$$\xi_t = -(g_1(\xi)\xi_{xxx})_x - (g_2(\xi)\xi_x)_x, \tag{1.10}$$

where g_1 and g_2 are typically polynomials, rather that (1.9) or (1.8), and much work has appeared in this direction [2, 12]. In particular, under suitable assumptions it has been demonstrated that three different types of steady states may occur for (1.10), namely constant states, positive periodic states, and compactly supported droplet states, and that the lowest energies are attained by the droplet states. Interesting enough, in the analysis of Mitlin [15], the possibility of droplet states existed but was not investigated. Seemingly, thus, compactly supported droplet solutions are a common feature to many of these types of studies, and are worthy of further attention. Recently an analysis of 'touchdown' or compactly supported steady state solutions with acute contact angles was considered in Laugesen & Pugh [13] for (1.10) where g_2 was allowed to be possibly singular at $\xi = 0$. However, for g_1 and g_2 which would correspond to the assumptions of (1.9) with disjoining pressure as singular as in (*i*) (*ii*), and (*iii*), the arguments in Novick-Cohen [18, 19] show that there are no 'touchdown' solutions. We emphasize, though, that for singular disjoining terms such as we wish to consider, it is very desirable to consider compactly supported

droplets, as the singular forces have been included in order to model such effects as the creation of dry patches on an exposed surface [27]. Within the framework of the revised thin film equation (1.8), our analysis shows that steady state 'touchdown' solutions do exist if the notion of 'touchdown' solution is suitably generalized to permit the inclusion solutions which are not single-valued, and dynamic modelling of dry spot creation may prove to be possible within such a framework.

Let us outline some of the results of Novick-Cohen [18, 19] to provide a background for the present framework, and also because our analysis shall rely on some results given there. In Novick-Cohen [18], an analysis was undertaken for a droplet with uniform cross-section that was completely wetting, i.e. $\gamma = \gamma_{SV} - \gamma_{SL}$, and which rested on a platform and was in equilibrium with a surrounding bulk fluid bath. In this case it was shown that though there did not exist any single-valued minimizers, within the class of rectifiable functions there existed a unique minimizer which was bounded by vertical segments which for realistic parameter values were on the order of at most a few molecular layers, and whose maximal height, $\bar{\xi}$, satisfied Derjaguin's prediction [4]:

$$P'(\bar{\xi}) + G'(\bar{\xi}) = 0. \tag{1.11}$$

Note that equation (1.11) corresponds to setting $H = 0$ and $\lambda = 0$ in (1.6). Since the droplet is in equilibrium with a bulk fluid bath, the droplet mass is not constrained and the rationale for setting λ to zero is clear.

In Novick-Cohen [19] a partially wetting ($0 < \gamma_{SV} - \gamma_{SL} < \gamma$) droplet with a uniform cross-section was considered, which lied on a solid substrate and was not in equilibrium with a surrounding bulk fluid bath. Here, on the basis of the results of Novick-Cohen [18], the analysis was initiated without constraining the class of admissible profiles to be single-valued. Rather we considered profiles bounded by rectifiable curves within the framework of a parametric generalization of the minimization problem, given below as **Problem PI**. More specifically, let Hypothesis HI be defined as follows:

Hypothesis HI: $f \in C^2(R^+, R^+)$ and

(i) $f + 1 > 0$,

(ii) $\lim_{\xi \to \infty} f' > 0$,

(iii) $\lim_{\xi \to 0} \xi^{p+2} f' = -q$, where $p \geqslant 0$ and $q > 0$ are (finite) constants,

(iv) $f'' > 0$.

We refer to q as the effective Hamaker constant.

We may state Problem PI in terms of Hypothesis HI as

Problem PI: Minimize $\mathbf{J} = \mathbf{J}[x, \xi]$, where

$$\mathbf{J} = \int_0^T [(\dot{x}^2 + \dot{\xi}^2)^{\frac{1}{2}} + f(\xi)\dot{x}]\, dt, \tag{1.12}$$

and where f satisfies **Hypothesis HI**, over all admissible configurations (x, ξ),

$$(x, \xi) = \{(x(t), \xi(t)),\ 0 \leqslant t \leqslant T\} \in \mathscr{S},$$

where $\mathscr{S}$ is the class of rectifiable curves which begin and end on the underlying solid

https://doi.org/10.1017/S0956792501004478 Published online by Cambridge University Press

substrate (i.e., $\xi(t) \geqslant 0$ for $0 < t < T$, and $\xi(0) = \xi(T) = 0$), which satisfy the mass constraint

$$\mathbf{m}[\xi] = \int_0^T \xi \dot{x}\, dt = m. \tag{1.13}$$

Here **J** and **m**, as defined, correspond respectively to a dimensionless free energy and a dimensionless mass per unit length (area) constraint, and the droplet density has been assumed to be uniform. Similarly f represents a dimensionless energy density summing the effects of the wetting energy, the gravitational potential, and the disjoining or generalized disjoining pressure. Though only the repulsive disjoining pressure $P(\xi) = \hat{A}\xi^{\alpha}$, $\hat{A} > 0$ was specifically mentioned in Novick-Cohen [18, 19], we emphasize here that f satisfying Hypothesis HI can also represent a potential of limiting repulsive form such as (i)–(iii) given earlier if the effects of the attracting forces are sufficiently benign. We remark that it should be possible to study Problem PI for limiting repulsive forces within the framework of assumptions which are more general than those of Hypothesis HI, however the subsequent analysis could be more involved. The nondimensional version of our problem given above can be attained by employing γ to rescale the energy density. The height of a droplet with infinite mass, δ can be used to rescale x and ξ. This height can be specified as the unique solution to

$$f'(\delta) = \frac{f(\delta) + 1}{\delta}, \tag{1.14}$$

see the discussion in §2.2. For simplicity, we do not introduce a change of notation in passing to the dimensionless versions of x and ξ. Furthermore, $\rho\delta^2$ and δ^2 can be used to scale the mass per unit length and the droplet cross-sectional area which we shall denote by S_0, respectively. In terms of the simple attractive disjoining pressure, this would imply then that

$$f(\xi) = k\xi^2 + \frac{c}{\xi^{\alpha}} + b, \tag{1.15}$$

with $b = -S\gamma^{-1} = -\cos\beta$, where β is the classically predicted contact angle given in (1.4), $c = \hat{A}\gamma^{-1}\delta^{-\alpha}$, and $k = \frac{1}{2}\rho g\delta^2\gamma^{-1}$ where g is the gravitational constant. The height, δ, assumes the value $\sqrt{2(\gamma - S)/(\rho g)}$ when $\hat{A} = 0$, and increases monotonely with $\hat{A}$ for $\hat{A} > 0$; i.e.,

$$\delta \geqslant \sqrt{2(\gamma - S)/\rho g}. \tag{1.16}$$

Thus α, b, c, and k would be constants such that $\alpha \geqslant 1$, $|b| \leqslant 1$, $c \geqslant 0$, and $k \geqslant 0$.

It was proven by Novick-Cohen [19] in the context of Problem PI, that there existed a continuum of configurations with infinity large (positive) energies [19, Figure 1(a)], and as well as a continuum of configurations with infinity large (negative) energies [19, Figure 1(b)]. Since this implied that the straightforward minimization process was no longer viable, the classical minimization process was replaced by a comparative minimization process (originally developed in the context of optimal control [26]) known as minimization in the sense of overtaking, i.e.

Definition Let $(x^1, \xi^1), (x^2, \xi^2) \in \mathscr{S}$. For any $\epsilon > 0$ let

$$\mathbf{J}_{\epsilon}[x, \xi] := \int_0^T [(\dot{x}^2 + \dot{\xi}^2)^{\frac{1}{2}} + f(\xi)\dot{x}]\chi_{\epsilon}(t)dt$$

https://doi.org/10.1017/S0956792501004478 Published online by Cambridge University Press

where

$$\chi_\epsilon(t) = \begin{cases} 1 & \xi(t) \geqslant \epsilon \\ 0 & \text{otherwise.} \end{cases}$$

We say that

$$\mathbf{J}[x^1, \xi^1] \leqslant \mathbf{J}[x^2, \xi^2] \text{ in the sense of overtaking,}$$

if

$$\mathbf{J}_\epsilon[x^1, \xi^1] \leqslant \mathbf{J}_\epsilon[x^2, \xi^2],$$

for all $0 < \epsilon \leqslant \epsilon_0$ for some $\epsilon_0 > 0$.

It was demonstrated by Novick-Cohen [19] that profiles which were not convex, i.e. profiles such that the bodies bounded by the rectifiable curve and by the substrate below were not convex, could not be minimizers in the sense of overtaking. Moreover, it was shown that if profiles bulged out, i.e. were convex but contained a section along which $x(t) < x(0)$ or $x(t) > x(T)$, then their energy could be decreased further by slightly lowering the profiles in an appropriate way. Therefore minimization of Problem I in the sense of overtaking was proven to be equivalent to straightforward minimization within a more restricted class of admissible configurations. We state below the equivalent minimization problem as Problem PII:

Problem PII: Minimize (1.12) subject to (1.13) for functions f satisfying **Hypothesis HI** over all configurations $(x, \xi) \in \tilde{\mathscr{S}}$, where $\tilde{\mathscr{S}}$ is the subset $\mathscr{S}$ which satisfies additionally that $x(0) \leqslant x(t) \leqslant x(T)$ for all $t \in [0, T]$.

It can be concluded from Theorem 4.2 in Novick-Cohen [19]

Theorem (I) *There exists a minimizer* (*possibly non-unique*) *to Problem II* (*or equivalently to Problem I in the sense of overtaking.*) *Such a minimizer* cannot *to be single-valued; more specifically, it necessarily contains a convex interior single-valued section bounded on either end by vertical segments of finite non-zero height.*

Thus while the earlier analysis for the behavior of completely wetting droplets in equilibrium with a bulk fluid reservior seemed complete, the analysis for partially wetting droplets not in equilibrium with a bulk fluid reservoir left open the question of uniqueness. Moreover, the appearance of vertical segments is seemed counterintuitive and unsatisfactory. In the present paper these issues are, for the most part, resolved. This is accomplished in two main steps. In §2, we prove

Theorem (A) *There exists a unique solution to Problem II. It is, moreover, symmetric about its center.*

In §3, we discuss in what sense the predictions of Youngs law are preserved despite the appearance of vertical segments, giving conditions which guarantee that the height of the vertical segments are very small relative to the overall height of the droplet. In particular, the results in §3 indicate that

Theorem (B) *For a droplet with cross-sectional area S_0 and with a free energy density given in terms of a dimensional height, ξ, as $\frac{1}{2}\rho g\xi^2 + \hat{A}\xi^{-\alpha} - S$, where $0 < \gamma - S$, if*

$$N_0 := \left(1 - \frac{2\gamma}{\rho g S_0}\right)\left[\frac{1}{(1+\alpha)\hat{A}}\left(\frac{2}{\rho g}\right)^{\alpha/2}(\gamma - S)^{\frac{\alpha+2}{2}}\right]^{\frac{1}{2+\alpha}} \gg 1, \tag{1.17}$$

then the effective contact angle, $\tilde{\beta}$, closely approximates Young's angle, β.

Some typical values of N_0 are listed in Table 2.

The proof of Theorem A, given in §2, is inherently constructive. First, in §2.1, relying on the results of Novick-Cohen [19], we demonstrate (Lemma 1) that it suffices to consider droplet profiles which are symmetric about their center. There afterwards a unique explicit representation is given (Theorem 2) for the left half of the unique droplet profile which is energy minimizing among all droplet profiles characterized by a given three values of the parameters A, B, and r, where A, B, and r which denote respectively the height of the bounding vertical segments, the maximum height of the droplet, and the half width of the droplet, i.e. half the length of the support of the droplet. This in turn allows a reduction of Problem II to the finite dimensional problem of identifying the optimal parameters A, B, and r, which is treated in §2.2. Via Theorems 3 and 4, it is proven that there exists a unique minimizing triplet (A, B, r) to the finite dimensional minimization problem. Lemma 1 and Theorems 2, 3 and 4 now imply Theorem A.

In §3, we consider Problem II in conjunction with Hypothesis HI*, which is somewhat more restrictive than Hypothesis HI.

Hypothesis HI*: $f(\xi) = \bar{f}(\xi) + c\xi^{-\alpha} + b$, where $\alpha > 1$, $c \geqslant 0$, $-1 < b < 0$, and $f(\xi) + 1 > 0$ for all $\xi > 0$. Moreover, $\bar{f}(\xi) \in C(R^+, R)$ satisfies (a) $\bar{f}(0) = 0$, (b) $\bar{f}'(0) > 0$, and (c) $0 < K_1 \leqslant \bar{f}''(\xi) < K_2$ for $\xi > 0$.

Note that $f(\xi)$ as given in (1.15) satisfies Hypothesis HI*, as would $f(\xi)$ of the form implied by (ii) for suitable values of the parameters. The assumption $-1 < b < 0$ arises as we wish to focus on the partial wetting case in which $0 < \beta < \frac{\pi}{2}$, see (1.4). In this context we prove (Theorem 9) that Young's law prediction for the contact angle hold 'at a suitable distance' from the edge of the droplet when measured according to an inscribed circle construction, if the ratio of the height of the bounding vertical segments to the maximum droplet height is sufficiently small. Moreover, we give sufficient conditions (Theorem 10) which guarantee that the ratio of the vertical segments to the overall droplet height is indeed small, for sufficiently large droplets and for sufficiently small values of $\frac{\hat{A}}{\gamma}\left(\frac{\rho g}{2\gamma}\right)^{\alpha/2}$ which is a scaled effective Hamaker constant. Theorems 9 and 10 together imply Theorem (B) stated earlier. Theorem 10 is also helpful in its own right in justifying the physicality of the predicted droplet profiles. We remark that it should be possible to prove results similar to Theorems 9 and 10 under less restrictive assumptions and hypotheses. In particular, some numerical results are presented which indicate that the ratio of the vertical segments to the overall droplet height may nevertheless be very small, even for extremely small masses.

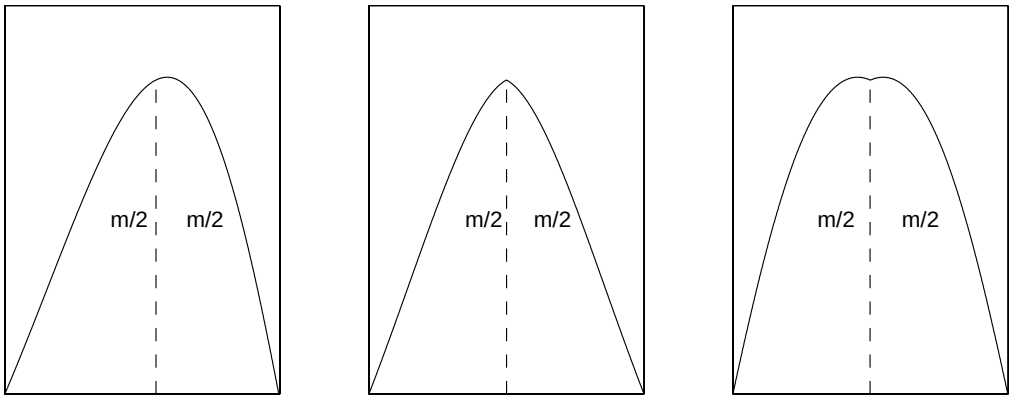

FIGURE 1. If an energy minimizing droplet for a given mean mass is nonsymmetric, then two nonidentical symmetric energy minimizing droplet profiles may be constructed which have the same mass and the same free energy as the nonsymmetric droplet profile.

2 The droplet profile

In this section we present the proof of Theorem (A); i.e., that there exists a unique minimizer to Problem PII, and that this minimizer is moreover symmetric about its center. From Theorem (I) which was stated in the Introduction, we know that all minimizers are necessarily bounded by vertical segments with positive height and contain an interior single-valued convex section. More precisely, we say that a minimizing profile $(x(t), \xi(t))$ is 'symmetric about its center', or more simply 'symmetric', if the vertical bounding segments on either side are of identical height and if $\xi(x) = \xi(2r-x)$ along the interior single-valued section, where $2r$ denotes the length of the support of the droplet.

Lemma 1 *In considering Problem PII, it suffices to consider symmetric droplet profiles only, since any nonsymmetric minimizing profile can be constructed by piecing together two halves of symmetric energy minimizing droplet profiles of equal mass.*

Proof The idea of the proof is given in Figure 1. A nonsymmetric minimizing droplet profile can be split into two halves via a vertical slicing, so that each of the halves contains half of the net mass. Each of the two halves must be possess exactly half of the net energy of the droplet, since otherwise the higher energy half could be replaced by a mirror image of the lower energy half, and the net energy of the droplet would be decreased. Thus each of the halves can be paired to a mirror image of itself to produce a symmetric droplet whose mass and energy are equal to that of the original minimizing droplet. Thus, the resultant two symmetric droplets will themselves be energy minimizers and will satisfy the mass constraint. Clearly, it follows than also that any nonsymmetric energy minimizing droplet can be constructed from the set of symmetric energy minimizers by gluing together the left half and the right half from two different symmetric minimizing droplet profiles. See also the discussion in Novick-Cohen [19]. □

https://doi.org/10.1017/S0956792501004478 Published online by Cambridge University Press

2.1 A finite dimensional reduction

Lemma 1 allows us to focus on the left half of a symmetric minimizing droplet profile, which according to Theorem (I) defines a characteristic triplet: (A, B, r), where A is the height of the vertical bounding segment, B is the maximal droplet height, and r is the droplet half-width ($r = x(T/2)$ in the terminology of Problem PII.) We demonstrate (Theorem 2, below) that if a droplet profile is energy minimizing for a given value of the mass, m, and the values of its characteristic triplet (A, B, r), $0 < A < B$, $r > 0$, are known, then the droplet profile is uniquely determined with the class $\tilde{\mathscr{S}}$.

Theorem 2 *Suppose that* $(x(t), \xi(t))$, $0 \leqslant t \leqslant T/2$ *describes the left half of an energy minimizing profile for a given value of* $m > 0$ *and for a given value of the characteristic triplet* (A, B, r) $0 < A < B$, $r > 0$. *Then along the interior single-valued convex section,* ξ *may be prescribed uniquely as a function of* x *as follows:*

$$\xi = \begin{cases} \Phi(x) & \text{for} \quad 0 < x < \beta(A,B,r) \\ B & \text{for} \quad \beta(A,B,r) \leqslant x \leqslant r \end{cases} \tag{2.1}$$

where

$$\beta(A,B,r) = \int_A^B R^{-\frac{1}{2}}(u)\,du, \tag{2.2}$$

$$R(u) = (f(B) + \lambda B + 1 - f(u) - \lambda u)^{-2} - 1, \tag{2.3}$$

and

$$\lambda = -\frac{f(B) + 1 - f(A)}{B - A}, \tag{2.4}$$

and where Φ *is defined implicitely by*

$$x = \int_A^{\Phi(x)} R^{-\frac{1}{2}}(u)\,du. \tag{2.5}$$

Remark According to Theorem 2, the energy minimizing droplet profile contains a 'flat top' with height B and length $r - \beta$. This apparent anomaly is soon resolved in Theorem 3, where it is proven that in fact $r - \beta = 0$.

Proof Clearly, by the construction $x(T/2) = r$. Employing a Lagrange multiplier, we can incorporate the mass conservation constraint and minimize:

$$\hat{\mathbf{J}} = \frac{\mathbf{J}}{2} + \lambda\left[\int_0^{T/2} \xi\dot{x}(t)\,dt - \frac{m}{2}\right];$$

i.e.

$$\hat{\mathbf{J}} = \int_0^{T/2} \left[f(\xi(t))\,\dot{x}(t) + \left(\dot{x}^2(t) + \dot{\xi}^2(t)\right)^{\frac{1}{2}} + \lambda\dot{x}(t)\left(\xi(t) - \frac{m}{2r}\right)\right] dt. \tag{2.6}$$

If, as we may assume without loss of generality, an arc-length parametrization is employed to describe the parametric curve $(x(t), \xi(t))$ (i.e. $(\dot{x}^2(t) + \dot{\xi}^2(t))^{1/2} = 1$), then since the droplet contains vertical segments of height A

$$x(t) = 0 \text{ for } t \in [0, A]. \tag{2.7}$$

https://doi.org/10.1017/S0956792501004478 Published online by Cambridge University Press

Moreover for $t \in (A, T/2]$, $(x(t), \xi(t))$ describes the left half of the interior single-valued convex portion of the energy minimizing droplet profile. Sufficient regularity is guaranteed by the convexity of the profile for $A < t < T/2$ for us to conclude that the Euler necessary condition must hold along this interior section [3, Theorem 2.2.i]. This implies (see Novick-Cohen [18, Lemma 4.5]) that along this section, the Euler necessary condition may be stated in terms of a single-valued function, $\xi = \xi(x)$, as

$$f(\xi) + (1 + \xi_x^2)^{-\frac{1}{2}} + \lambda\left(\xi - \frac{m}{2r}\right) = D, \quad x \in (0, r]$$

where D is a constant to be determined. Defining

$$C = D + \frac{\lambda m}{2r}, \tag{2.8}$$

we may conclude

$$f(\xi) + \lambda\xi + (1 + \xi_x^2)^{-\frac{1}{2}} = C, x \in (0, r] \text{ and } \xi(0) = A. \tag{2.9}$$

Note that $\xi(0)$ corresponds to the height of the vertical segment, A, and $\xi(r)$ corresponds to the maximal height of the droplet, B.

Since the profile is vertical for $0 < t < A$, and the form of the profile is determined by equation (2.9) for $A < t < T/2$, the parametric curve $(x(t), \xi(t))$ is certainly sufficiently regular to invoke the Erdman (necessary) corner condition [3, Theorem 2.2i] for $A/2 < t < A/2 + T/4$, and hence there can be no break in the profile derivative in this interval. In particular, we may conclude that

$$\xi_x(0) = \infty. \tag{2.10}$$

Since the droplet is symmetric and convex, in fact the parametric minimization problem can be equally well formulated for the whole droplet, taking the integral in (2.6) over the interval $[0, T]$. Thus, the Euler necessary condition and the Erdmann corner condition must hold for $T/4 + A/2 < t < 3T/4 - A/2$. Therefore,

$$\xi_x(r) = 0. \tag{2.11}$$

From (2.9), (2.10) and (2.11), it follows that

$$C = f(A) + \lambda A = f(B) + \lambda B + 1. \tag{2.12}$$

Following Novick-Cohen [19], (2.1)–(2.5) may be concluded from (2.9) and (2.12). □

Since ξ as given in Theorem 2 above is the unique minimizing left half profile of (2.6) for given values of A, B, and r, the global minimizer(s) may now be ascertained by substituting the profile as prescribed above back into (2.6) yielding $\hat{\mathbf{J}} = \hat{\mathbf{J}}(A, B, r)$, then minimizing $\hat{\mathbf{J}}$ over the domain $\mathscr{R}$, where

$$\mathscr{R} = \{A, B, r \,|\, 0 < A < B, r > 0\}.$$

This is accomplished in the next subsection.

https://doi.org/10.1017/S0956792501004478 Published online by Cambridge University Press

2.2 The optimal parameters A, B, r

Theorem 3 *In an energy minimizing profile for a given mass $m > 0$, the parameters A, B, and r must satisfy*

$$\frac{f(A)}{A} = \frac{f(B)+1}{B}, \tag{2.13}$$

$$\int_A^B \frac{\left|\frac{f(A)}{A}u - f(u)\right| u\,du}{\sqrt{1-\left(\frac{f(A)}{A}u - f(u)\right)^2}} = \frac{m}{2}, \tag{2.14}$$

$$\int_A^B \frac{\left|\frac{f(A)}{A}u - f(u)\right| du}{\sqrt{1-\left(\frac{f(A)}{A}u - f(u)\right)^2}} = r. \tag{2.15}$$

Moreover, $\beta(A, B, r) = r$.

Proof Let us assume that the parameters A, B and r are optimal. The corresponding energy minimizing droplet profile must have a vertical section of height A at $x = 0$, and a single-valued section which satisfies (2.1)–(2.5). Substituting (2.1)–(2.4) into (2.6), we obtain

$$\hat{\mathbf{J}} = A - \frac{\lambda m}{2} + (r-\beta)(f(B)+1+\lambda B) + \int_0^\beta \left[f(\Phi(x)) + \lambda\Phi(x) + \left(1+\Phi_x^2\right)^{\frac{1}{2}}\right] dx, \tag{2.16}$$

yielding $\hat{\mathbf{J}} = \hat{\mathbf{J}}(A, B, r)$, since $\lambda = \lambda(A, B)$ by (2.4). Differentiating (2.5) with respect to x and utilizing (2.2)–(2.3),

$$\hat{\mathbf{J}} = A - \frac{\lambda m}{2} + r(f(B)+1+\lambda B) + \int_A^B \frac{R^{\frac{1}{2}}(u)}{(1+R(u))^{\frac{1}{2}}}\,du. \tag{2.17}$$

Notice also that (2.12) implies the parametric constraint (2.13). It is easily verified that the conditions of **Hypothesis HI** imply that the optimal values of the parameters cannot lie on the boundary of the domain $\mathscr{R}$. Thus, we may assume that A, B, and r lie within the interior of $\mathscr{R}$, and $\hat{\mathbf{J}}$ must assume a local interior minimum at this set of values.

Differentiability of $\hat{\mathbf{J}}(A, B, r)$ within the domain $\mathscr{R}$ allows us to obtain a system of conditions defining the local minima by setting the partial derivatives of $J(A, B, r)$ equal zero and taking (2.13) into account. This gives

$$0 = \left[-\frac{m}{2} + Br - \int_A^B \frac{B-u}{R^{1/2}(u)}\,du\right]\left[\frac{f'(A)+\lambda}{B-A}\right], \tag{2.18}$$

$$0 = \left[-Ar + \frac{m}{2} + \int_A^B \frac{A-u}{R^{1/2}(u)}\,du\right]\left[\frac{f'(B)+\lambda}{B-A}\right], \tag{2.19}$$

$$0 = f(B) + 1 + \lambda B. \tag{2.20}$$

From (2.20) and (2.4), it follows that $\lambda = -\frac{f(A)}{A} = -\frac{f(B)+1}{B}$. Suppose now that $f'(A)+\lambda = 0$. This implies that $f'(A) = f(A)/A$. However, then the point $(A, f(A))$ would be located on a tangent to $f(\xi)$ which passes through the origin and the parametric constraint (2.13)

https://doi.org/10.1017/S0956792501004478 Published online by Cambridge University Press

could not be satisfied. Thus

$$f'(A) + \lambda \neq 0. \tag{2.21}$$

Suppose similarly that $f'(B) + \lambda = 0$. Then we obtain that $f'(B) = (f(B) + 1)/B$. By referring to equations (2.2)–(2.3), we see by examining the behavior of the integral in the neighborhood of $u = B$ that this would yield that $\int_A^B R^{-\frac{1}{2}}(u)\, du = \infty$. This, however, gives that $r = \infty$ (and $m = \infty$) and would correspond to a minimum on the boundary of $\mathscr{R}$. Since we have noted that there are no minima on the boundary of the domain $\mathscr{R}$, we conclude that

$$f'(B) - (f(B) + 1)/B \neq 0. \tag{2.22}$$

It follows now easily from (2.18) and (2.19), using (2.2), (2.21) and (2.22), that $\beta(A, B, r) = r$. From (2.2), (2.3) and (2.18), (2.14) and (2.15) are now obtained. □

Let us examine the system (2.13)–(2.15) for a given value of $m > 0$. Equation (2.15) can be viewed as determining r in terms of A and B. Note that the convergence of the integral in (2.15) is assured by convergence of integral in (2.14). It remains to verify whether equations (2.13)–(2.14) can be uniquely solved for A and B. That this is so is guaranteed by the following theorem:

Theorem 4 *If f satisfies Hypothesis HI, then for any $m > 0$ the system (2.13)–(2.14) has a unique solution.*

Proof Under the conditions of Hypothesis HI, clearly there exists a unique tangent to the curve $y = f(\xi) + 1$ that pass through $(0, 0)$. Let us denote the point of tangency by $(B_\infty, f(B_\infty) + 1)$, and the first intersection of the tangent constructed above with the curve $y = f(u)$ by $(A_\infty, f(A_\infty))$ – see Figure 2.

It follows from the construction that

$$\frac{f(A_\infty)}{A_\infty} = f'(B_\infty) = \frac{f(B_\infty) + 1}{B_\infty}. \tag{2.23}$$

Let us now take $A > 0$ to be given, and attempt to solve (2.13) for B as a function of A. In this regard we have

Lemma 5 *For $A \in (0, A_\infty)$, there exists a unique value of B, $B = B^*(A)$, such that* (2.13) *is satisfied and the integral in* (2.14) *is real and convergent. Moreover,* $\lim_{A \to A_\infty} B^*(A) = B_\infty$. *For $A \in (A_\infty, \infty)$, there are no solutions to* (2.13) *such that $A < B$.*

Proof From the construction and Hypothesis HI it is easy to see that for any $A \in (0, A_\infty)$, the line connecting $(0, 0)$ with $(A, f(A))$ intersects the curve $y = f(\xi) + 1$ to the right of $(A, f(A))$ in precisely two points. Let us denote the values of ξ where the two intersections occur by B and B', with $B < B'$. Thus for $A \in (0, A_\infty)$, (A, B) and (A, B') constitute the only solutions to (2.13). Furthermore, for $A > A_\infty$, the line connecting $(0, 0)$ with $(A, f(A))$ does not intersect the curve $y = f(\xi) + 1$, hence there are no solutions to (2.13) for $A > A_\infty$. Note, further that by the construction, $f(A)/A < (f(\xi) + 1)/\xi$ for $A < \xi < B_1$ and $f(A)/A > (f(\xi) + 1)/\xi$ for $B < \xi < B'$. By considering

https://doi.org/10.1017/S0956792501004478 Published online by Cambridge University Press

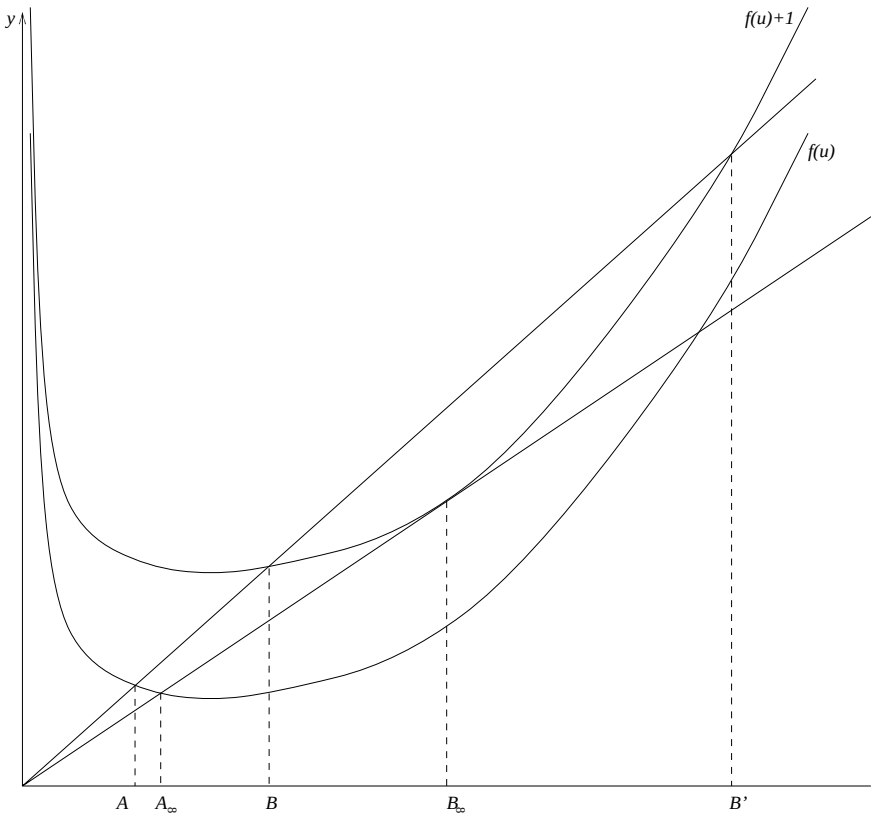

FIGURE 2. A sketch of the A_∞-B_∞ construction. Here A and B satisfy (2.13) and correspond to the height of the bounding vertical segments and to the overall height, respectively, for an energy minimizing profile with finite mass. A_∞ and B_∞ satisfy (2.23) and have the same connotation as A and B, except that they refer to the limiting values of these parameters as the mass approaches infinity. See §2.2.

the denominator of the integrand in (2.14), this can be seen to imply that with B as given by the construction as the upper limit of integration, the integral on the left hand side of (2.14) is real and convergent whereas if B' is used as the upper limit of integration, the integral on the left hand side is necessarily complex. Therefore, for $A \in (0, A_\infty)$ there exists a unique $B = B^*(A)$, given by B of the construction, for which the integral in (2.14) is real and convergent. From the construction, it also follows that $\lim_{A \to A_\infty} B^*(A) = B_\infty$. □

For $A \in (0, A_\infty)$, we define

$$\phi(A) = \int_A^{B^*(A)} \frac{\left| \dfrac{f(A)}{A} u - f(u) \right| u \, du}{\sqrt{1 - \left(\dfrac{f(A)}{A} u - f(u) \right)}}.$$

Solveability of the system (2.13)–(2.14) is now resolved by examining the behavior of $\phi(A)$ for $A \in (0, A_\infty)$.

https://doi.org/10.1017/S0956792501004478 Published online by Cambridge University Press

Lemma 6 *$\phi(A)$ is a monotone increasing function of A for $A \in (0, A_\infty)$.*

Proof of Lemma 6

Claim 7 If f satisfies Hypothesis HI, then $\frac{\partial}{\partial \xi}(\frac{f(\xi)}{\xi}) < 0$ for $\xi \in (0, A_\infty]$, and $\frac{\partial}{\partial \xi}(\frac{f(\xi)+1}{\xi}) < 0$ for $\xi \in (0, B_\infty]$.

Proof Let $v(\xi) = \xi f'(\xi) - f(\xi)$. By Hypothesis HI, $v'(\xi) = \xi f''(\xi) > 0$ for $\xi > 0$. Using (2.23),

$$v(A_\infty) = A_\infty f'(A_\infty) - f(A_\infty) = A_\infty(f'(A_\infty) - f'(B_\infty)).$$

It follows from the convexity of f that $v(A_\infty) < 0$. Therefore, $v(\xi) < 0$ for all $\xi \in (0, A_\infty)$. Similarly, it follows from (2.23) that $v(B_\infty) = 1$. Hence $v(\xi) - 1 < 0$ for $\xi \in (0, B_\infty)$. Noting now that

$$\frac{\partial}{\partial \xi}\left(\frac{f(\xi)}{\xi}\right) = v(\xi)/\xi^2 \text{ and } \frac{\partial}{\partial \xi}\left(\frac{f(\xi)+1}{\xi}\right) = (v(\xi) - 1)/\xi^2,$$

the claim follows. □

Let us define

$$g(A, \xi) = \frac{f(A)}{A}\xi - f(\xi). \tag{2.24}$$

It follows from Claim 7 that $\frac{f(A)}{A} > \frac{f(A_\infty)}{A_\infty}$ for $A \in (0, A_\infty)$, and clearly $f'(\xi) \leqslant \frac{f(A_\infty)}{A_\infty}$ for any $\xi \in (0, B_\infty]$. Therefore,

$$\frac{\partial g}{\partial \xi}(A, \xi) = \frac{f(A)}{A} - f'(\xi) > 0 \text{ for } A \in (0, A_\infty),\ \xi \in (0, B_\infty]). \tag{2.25}$$

Since $g(A, A) = 0$ and $g(A, B) = 1$ if $A \in (0, A_\infty)$ and $B = B^*(A)$ as prescribed in Lemma 5, we obtain by virtue of (2.25) that for any $A \in (0, A_\infty)$, there exists an inverse function $u(A, g)$ such that $u(A, 0) = A$, $u(A, 1) = B$ and which is differentiable and monotone increasing with respect to g, for $g \in (0, 1)$. Therefore, we may rewrite (2.14) in the form

$$\int_A^B \frac{\left|\frac{f(A)}{A}u - f(u)\right| u\, du}{\sqrt{1 - \left(\frac{f(A)}{A}u - f(u)\right)^2}} = \int_0^1 \frac{g}{\sqrt{1-g^2}} u(A, g)\, u_g(A, g)\, dg. \tag{2.26}$$

It follows from Claim 7 that both $g(A, \xi)$ and $g_\xi(A, \xi)$ are decreasing functions of A for $\xi > 0$ and $A \in (0, A_\infty)$, so both $u(A, g)$ and $u_g(A, g)$ are increasing functions of A. Since g in (2.26) is an independent variable and $u(A, g)$ and $u_g(A, g)$ are increasing functions of A, the integral is also increasing function of A. □

Lemma 8 *$\phi(A) \to 0$ as $A \to 0$, and $\phi(A) \to \infty$ as $A \to A_\infty$.*

Proof By (2.25), for $A \in (0, A_\infty)$, $g_\xi(A, \xi)$ is strictly positive and continuous for $\xi \in (0, B_\infty]$, and by Hypothesis HI, $g_\xi(A, \xi) \to \infty$ as $\xi \to 0$. Hence $u_g(A, g)$ is bounded and continuous for $A \in (0, A_\infty)$, $g \in [0, 1]$. Let $A_0 \in (0, A_\infty)$ be arbitrary, and let us define

$$\alpha := \max_{g \in [0,1]} u_g(A_0, g). \tag{2.27}$$

https://doi.org/10.1017/S0956792501004478 Published online by Cambridge University Press

Recall that we have seen in the proof of Lemma 6 that $u_g(A, g)$ is an increasing function of A for $A \in (0, A_\infty)$ and $g \in (0, 1)$. Hence for any $A \in (0, A_0]$ and $g \in [0, 1]$, $u_g(A, g) \leqslant \alpha$. Therefore, by (2.26), for $A \in (0, A_0]$

$$\phi(A) \leqslant \alpha \int_0^1 \frac{g}{\sqrt{1-g^2}} u(A, g)\, dg \leqslant \alpha \max_{g\in[0,1]} (u(A, g)) \int_0^1 \frac{g}{\sqrt{1-g^2}}\, dg = \alpha B(A). \tag{2.28}$$

Since clearly $\lim_{A\to 0} B(A) = 0$, it follows that $\phi(A) \to 0$ as $A \to 0$.

Noting $B(A_\infty) = B_\infty$ and $f'(B_\infty) = \frac{f(A_\infty)}{A_\infty}$, it is easy to check upon examining the behavior of the integrand in (2.14) near its upper limit, that the integral diverges as $A \to A_\infty$. Therefore, $\phi(A) \to \infty$ as $A \to A_\infty$. □

From Lemma 6 and Lemma 8, it follows that for any $m > 0$, there exists a unique $A^* \in (0, A_\infty)$ such that $\phi(A^*) = m/2$. Therefore, by Lemma 5, $(A, B) = (A^*, B^*(A^*))$ constitutes the unique solution of (2.13)–(2.14), and Theorem 4 is proven. □

Combining the results of Lemma 1, Theorem 2, Theorem 3 and Theorem 4 yields a proof of Theorem (A) as stated in the Introduction.

Remark It also follows from Lemmas 6 and 8 that B_∞ is the height of a droplet with infinite mass. From the normalization introduced in (1.14) and (2.23), we know that $B_\infty = 1$.

See Figure 3 for a numerical plot of an energy minimizing profile for a simple repulsive disjoining pressure.

In the plot the parameter values $S = 0.025\ \mathrm{J\,m^{-2}}$, $\gamma = 0.05\ \mathrm{J\,m^{-2}}$, $\rho = 2 \times 10^{-3}\ \mathrm{kg\,m^{-3}}$, $S_0 = 2 \times 10^3\ \mathrm{m^2}$ (cross-sectional area), $\alpha = 2$, and $\hat{A} = 10^{-22}\ \mathrm{J}$ have been assumed.

3 The contact angle

Having established uniqueness and having derived an implicit expression for the energy minimizing droplet profile, we now turn to see what can be said about the contact angle and the height of the vertical bounding segments relative to the overall droplet height.

According to (2.10), the contact angle is always equal to $\frac{\pi}{2}$ in the present context, if it is measured at the point of contact. Experimental measurements typically reflect an 'averaging' or curve fitting of the shape of the droplet profile near the contact point, not a TEM-type microscopic contact angle[1]. We too predict a type of 'averaged' angle by approximating the droplet profile, near but not at the contact point by an inscribed circle. This corresponds in a sense to looking as an intermediate angle as has been considered

[1] TEM, or electron transmission microscopy [6], can be used when atoms stay still long enough to be imaged, as in solids. Such techniques permit resolution on an angström scale, as opposed to $\approx 10\ \mu$ level resolution which can be achieved with low resolution optical microscopy and video imaging. Recently resolution on the scale of $10 - 100$ nm has also been reported in the context of thin liquid crystal and liquid metal films using SFM [10], though these methods are based on thickness measurements and are not directly applicable for finding the fine structure at the very edge of a droplet.

https://doi.org/10.1017/S0956792501004478 Published online by Cambridge University Press

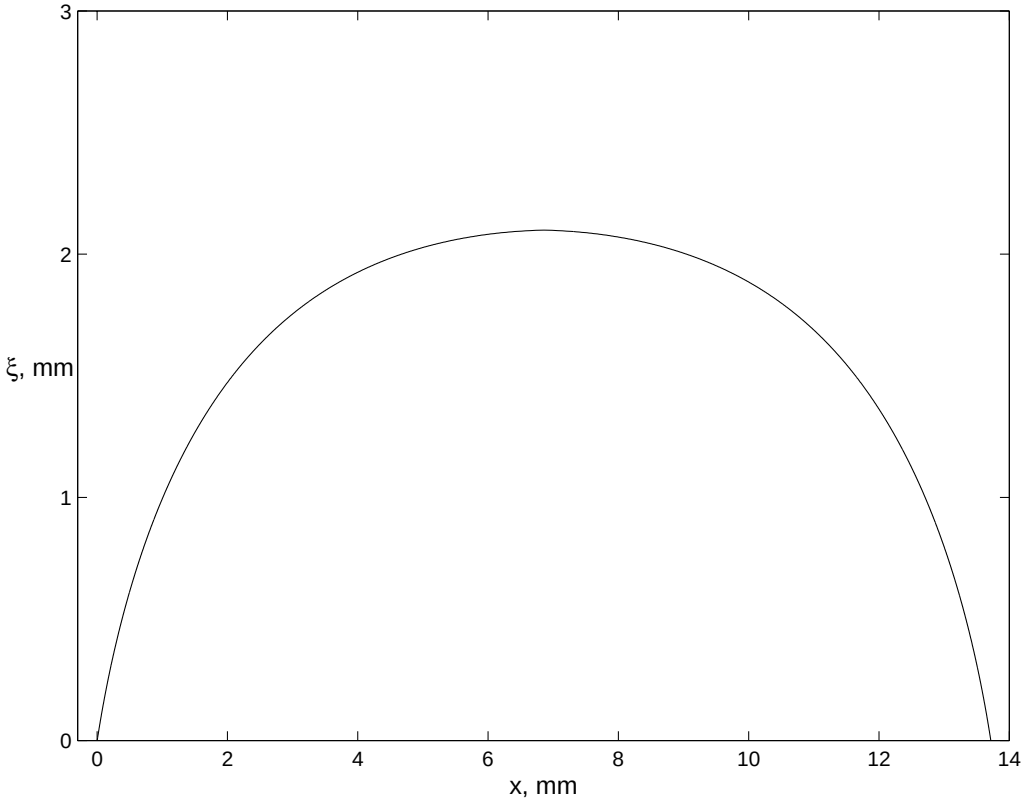

FIGURE 3. A numerically plotted energy minimizing droplet profile, where the parameter values $\gamma = 0.05\, Jm^{-2}$, $S = 0.025\ \mathrm{J\,m^{-2}}$, $S_0 = 2 \times 10^{-5}\ \mathrm{m^2}$, $\alpha = 2$, and $\hat{A} = 10^{-22}$ J have been assumed. While the overall height of the droplet is roughly equal to 2.1 mm, the height of the vertical bounding segments is roughly equal to .63 $\mathring{A}$ and thus far below the resolution of the plot.

in the context of dynamic contact angles [5]. We approximate the contact angle by the angle which is made by the inscribed tangent circle and the underlying substrate at their point of intersection. If this approximation is to be reasonable, it must be relatively independent of the precise location of the inscribed circle construction within the droplet profile. We bring to the reader's attention that the droplet profile need not be circular in order for the approximation to be accurate; whenever the droplet energy density is nonsingular then our proposed measurement reduces to the classical prediction – see (3.5) below.

Let us see the implications of such an approximation. From (2.5) and (2.24), we obtain that for $A < \xi < B$

$$x(\xi) = \int_A^{\xi} \frac{g(A, u)}{\sqrt{1 - g^2(A, u)}}\, du, \tag{3.1}$$

where A, we recall, denotes the height of the vertical bounding segments and B denotes the overall droplet height. Using (3.1), the mean curvature of the profile as a function of

https://doi.org/10.1017/S0956792501004478 Published online by Cambridge University Press

height, $H(\xi)$ may be easily computed to be

$$H(\xi) = \frac{x''(\xi)}{\left(1 + x'^2(\xi)\right)^{\frac{3}{2}}} = \frac{f(A)}{A} - f'(\xi). \tag{3.2}$$

Note that $\sigma(\xi) = 1/H(\xi)$ denotes the radius of curvature of the profile surface at height ξ. We need now an analytic expression for $\tilde{\beta}$, the angle between the x axis and the circle of radius σ that passes through the point $(x(\xi_0), \xi_0)$ and is tangent to the droplet profile $\xi = \xi(x)$, which is our proposed approximant for an effective contact angle when $(x(\xi_0), \xi_0)$ is appropriately chosen. It is easy to check that

$$\tilde{\beta} = \arccos(\xi_0 f'(\xi_0) - f(\xi_0)). \tag{3.3}$$

Suppose, for a moment, we consider (3.3) in the classical case in which all singular van der Waals forces are neglected and only gravitational and surface energy effects are taken into account. In the present notation this would imply that

$$f(\xi) = k\xi^2 + b. \tag{3.4}$$

Then substituting (3.4) into (3.3) yields

$$\tilde{\beta} = \arccos(k\xi_0^2 - b).$$

If ξ_0 is measured sufficiently close to the droplet edge, then $0 < \xi_0 \ll 1$ and a Taylor expansion about 0 gives

$$\tilde{\beta} = \arccos(-b) - \tfrac{1}{2}k(1 - b^2)^{-\frac{1}{2}}\bar{\xi}^2 \text{ for some } 0 < \bar{\xi} < \xi_0.$$

Thus, if $-1 < b < 0$ as we have assumed throughout, then by (1.4)

$$\tilde{\beta} = \beta + \mathcal{O}(\xi_0^2) \tag{3.5}$$

where β is the classical contact angle. In particular, we see that the prediction for the effective contact angle is relatively insensitive to the precise point at which it is measured.

We wish now to connect $\tilde{\beta}$ with the classical contact angle, β, when the effects of singular van der Waals forces are included in f. In this section we shall limit our considerations for simplicity to functions f of the form

$$f(\xi) = \bar{f}(\xi) + \frac{c}{\xi^\alpha} + b \tag{3.6}$$

which satisfies **Hypothesis HI*** of the Introduction, and recall that such functions can reflect disjoining pressures of type *ii*) for suitable values of the parameters. We focus now on finding an acceptable height at which to make measurements. Let us assume for the moment that the height of the vertical bounding segments comprises only a fraction of the overall droplet height, i.e.

$$A \ll B. \tag{3.7}$$

Intuitively, it would be surprising if (3.7) were not to hold. Indeed, in Minkov [14], droplet profiles were calculated numerically when the function f was assumed to be given by (1.15) and a series of realistic values were taken for the parameters b, α, c, and m. (Figure 3, given earlier, was produced on the basis of these calculations.) A, B, as well as the ratio $N = B/A$ were evaluated. See Table 1, where it can be seen that for all of the tabulated

https://doi.org/10.1017/S0956792501004478 Published online by Cambridge University Press

values, N was found to be in the range $\sim 10^3$–10^7. Since experimentally to has not been possible to resolve a finite 'droplet side height', this would indicate that N must be greater than (the overall droplet height)/(the limits of microscopic resolution), i.e. say roughly $\mathrm{mm}/10\,\mu = 3 \times 10^2$, which is in line with our predictions. We shall further substantiate assumption (3.7) theoretically in Theorem 10 and Corollary 11 for the case of sufficiently large masses, though the data in Table 1 indicates that (3.7) may hold even for quite small droplets, i.e. droplets with cross-sectional area on the order of 2×10^{-9} m^2. The assumption (3.7) make it possible for us to consider ξ_0 such that $A \ll \xi_0 \ll B$ and since by our choice of scaling $B < B_\infty = 1$, this implies, furthermore, that $0 < \xi_0 \ll 1$. In this context, we now demonstrate that (3.3) does indeed constitute an approximation to the classical contact angle.

Theorem 9 *If f satisfies Hypothesis HI* and $A \ll \xi_0 \ll B$, then* $\cos\tilde{\beta} = -b + \mathcal{O}(\xi_0^2) + \mathcal{O}(A/B)$.

Proof Let us substitute (3.6), the assumed form for f, into the parametric constraint (2.13), then solving for c

$$c = A^{\alpha+1}\left[\frac{\bar{f}(B)+b+1}{B} - \frac{\bar{f}(A)+b}{A}\right]\left(1 - \left[\frac{A}{B}\right]^{\alpha+1}\right)^{-1}.$$

Since $0 < A \ll B < 1$ and by the assumptions of **Hypothesis HI*** on $\bar{f}$, we obtain that

$$c = A^{\alpha}\left[\frac{A}{B}\right](\bar{f}(B)+b+1) - A^{\alpha}(\bar{f}(A)+b) + A^{\alpha}\cdot\mathcal{O}\left(\left[\frac{A}{B}\right]^{\alpha+1}\right). \tag{3.8}$$

Returning now and substituting (3.6) into (3.3)

$$\tilde{\beta} = \arccos\left(\xi_0\bar{f}'(\xi_0) - b - \bar{f}(\xi_0) - \frac{c(1+\alpha)}{{\xi_0}^{\alpha}}\right).$$

Using (3.8) yields

$$\tilde{\beta} = \arccos\left(\xi_0\bar{f}'(\xi_0) - b - \bar{f}(\xi_0) - \frac{A^{\alpha}}{\xi_0^{\alpha}}(1+\alpha)\left[\frac{A}{B}(\bar{f}(B)+b+1) - (\bar{f}(A)+b)\right] + \mathcal{O}\left(\left[\frac{A}{\xi_0}\right]^{\alpha}\cdot\left[\frac{A}{B}\right]^{\alpha+1}\right)\right).$$

From the assumptions on $\bar{f}$ and since $0 < A \ll \xi_0 \ll B < 1$, this implies that

$$\tilde{\beta} = \arccos(-b + \mathcal{O}(\xi_0^2) + \mathcal{O}((A/\xi_0)^{\alpha})).$$

Thus, by (1.4) and since $-1 < b < 0$

$$\tilde{\beta} = \beta + \mathcal{O}(\xi_0^2) + \mathcal{O}((A/\xi_0)^{\alpha}).$$

□

We turn now to state and prove Theorem 10.

Theorem 10 *Let f be assumed to satisfy Hypothesis HI*, let K_1, K_2 correspond to the bounds prescribed in Hypothesis HI*, and let $\xi_{\min}$ denote the (unique) minimizer of f. Suppose, moreover, that $\frac{\overline{K}m}{2} > 1$ where $\overline{K} = \liminf_{0<\xi<B_\infty} f''(\xi)$.*

https://doi.org/10.1017/S0956792501004478 Published online by Cambridge University Press

Table 1. *$B/A\,(=N)$ vs. physical parameters*

γ, J m^{-2}	ρ, kg m^{-3}	α	$\hat{A}$, J	S_0, m^2	S/γ	B/A
0.05	10^3	2	10^{-22}	10^{-5}	0	1.9×10^5
0.05	10^3	2	10^{-22}	10^{-5}	0.5	3.3×10^7
0.05	10^3	2	10^{-22}	10^{-6}	0	8.7×10^4
0.05	10^4	2	10^{-21}	10^{-6}	0	3.9×10^4
0.05	10^5	2	10^{-19}	$2 \cdot 10^{-9}$	0	1.0×10^3

Table 2. *δ, $km = (g\rho S_0)/(2\gamma)$, $ck^{\alpha/2} = (\hat{A}/\gamma)\cdot(\rho g/2\gamma)^{\alpha/2}$ and N_0 vs. physical parameters for $\alpha = 2$*

γ, J m^{-2}	ρ, kg m^{-3}	S/γ	$\hat{A}$, J	S_0, m^2	δ, m	km	$ck^{\alpha/2}$	N_0
0.05	10^3	0	10^{-22}	10^{-5}	3.2×10^{-3}	0.98	1.96×10^{-16}	-1.3×10^2
0.02	10^3	0.5	10^{-21}	10^{-5}	1.4×10^{-3}	2.5	4.9×10^{-15}	9.7×10^2
0.05	1.3×10^4	0	10^{-19}	10^{-6}	9×10^{-4}	1.3	2.54×10^{-12}	1.4×10^2
0.05	1.3×10^4	0.5	10^{-19}	10^{-5}	6×10^{-4}	12.7	2.54×10^{-12}	5.5×10^2
0.02	0.8×10^3	0.5	10^{-19}	10^{-5}	2.3×10^{-3}	2.0	3.92×10^{-13}	2.7×10^2
0.05	10^5	0	10^{-19}	$2 \cdot 10^{-9}$	3×10^{-4}	0.02	1.96×10^{-11}	-1.7×10^4

(i) *If $f(\xi_{\min}) < 0$, then*

$$N > \left(1 - \frac{2}{\overline{K}m}\right)\left(\frac{K_1}{\alpha c}\right)^{\frac{1}{2+\alpha}}. \tag{3.9}$$

(ii) *If $f(\xi_{\min}) > 0$, $K_2 < 2K_1$, and $c < (K_2 - \frac{1}{2}K_1)^{-\alpha/2}(1+b)^{\frac{2+\alpha}{2}}$, then*

$$N > \left(1 - \frac{2}{\overline{K}m}\right)\left[\frac{K_1 - \frac{1}{2}K_2}{(1+\alpha)c}\right]^{\frac{1}{2+\alpha}}. \tag{3.10}$$

Theorem 10 is important not only because it allows us to demonstrate that Youngs' law effectively holds, but also because it can guarantee that the vertical segments are very small. Theorems 9 and 10 together imply that the net effect of the vertical segments is often neglible.

To understand the physical implications of Theorem 10, we give below a corollary implied by Theorem 10 when f has the specific form given by (1.15) which corresponds to a simple repulsive disjoining pressure.

Corollary 11 *If $f(\xi) = k\xi^2 + c\xi^{-\alpha} + b$, with $\alpha \geqslant 1$, $-1 < b < 0$, $c, k > 0$ and $km > 1$,*

(i) *and if*

$$ck^{\alpha/2} \leqslant (-b)^{\frac{2+\alpha}{2}}\left[\left(\frac{\alpha}{2}\right)^{\frac{2}{2+\alpha}} + \left(\frac{2}{\alpha}\right)^{\frac{\alpha}{2+\alpha}}\right]^{-\frac{(2+\alpha)}{2}},$$

then

$$N > \left(1 - \frac{1}{km}\right)\left(\frac{2k}{\alpha c}\right)^{\frac{1}{2+\alpha}}, \tag{3.11}$$

https://doi.org/10.1017/S0956792501004478 Published online by Cambridge University Press

(ii) *and if*

$$(-b)^{\frac{2+\alpha}{2}}\left[\left(\frac{\alpha}{2}\right)^{\frac{2}{2+\alpha}}+\left(\frac{2}{\alpha}\right)^{\frac{\alpha}{2+\alpha}}\right]^{-\frac{(2+\alpha)}{2}}<ck^{\alpha/2}<(1+b)^{\frac{2+\alpha}{2}},$$

then

$$N>\left(1-\frac{1}{km}\right)\left(\frac{k}{(1+\alpha)c}\right)^{\frac{1}{2+\alpha}}. \tag{3.12}$$

The requirement that $km>1$ can be stated in terms of the original physical parameters as $(\frac{\rho g S_0}{2\gamma})>1$, i.e. gravitational effects dominate over surface tension effects. This condition may be satisfied by considering sufficiently large droplets. Conditions (i) and (ii) require that $ck^{\alpha/2}$ be sufficiently small, which implies in terms of the original physical parameters that $\frac{\hat{A}}{\gamma}\left[\frac{\rho g}{2\gamma}\right]^{\alpha/2}$ must be sufficiently small. Since classical analysis predicts that $A=0$ $(N=\infty)$ when $\hat{A}$ vanishes and van der Waals forces are neglected, it seems reasonable to expect that an upper bound on $c\left(=\frac{\hat{A}}{\gamma\delta^{\alpha}}\leqslant\frac{\hat{A}}{\gamma}\left[\frac{2(\gamma-S)}{\rho g}\right]^{\alpha/2}\right)$ can guarantee that $N\gg 1$. For ease of interpretation, we give below a similar corollary stated in term of dimensional variables and quantities.

Corollary 12 *If the dimensional free energy density is given by* $\frac{1}{2}\rho g\xi^2+\hat{A}\xi^{-\alpha}-S$, *where* ξ *is a dimensional height and* $0<\gamma-S$, *and if* (a) $\rho g S_0>2\gamma$ *and* (b) $(\frac{1}{2}\rho g)^{\alpha/2}\hat{A}<(\gamma-S)^{\frac{2+\alpha}{2}}$, *then* $N>N_0$ *where*

$$N_0=\left(1-\frac{2\gamma}{\rho g S_0}\right)\left[\frac{1}{(1+\alpha)\hat{A}}\left(\frac{2}{\rho g}\right)^{\alpha/2}(\gamma-S)^{\frac{\alpha+2}{2}}\right]^{\frac{1}{2+\alpha}}.$$

Proof The proof is based on part *ii*) of Corollary 11, and the estimate

$$\frac{k}{c}=\frac{\rho g}{2\hat{A}}\delta^{2+\alpha}\geqslant\frac{\rho g}{2\hat{A}}\left[\frac{2(\gamma-S)}{\rho g}\right]^{\frac{2+\alpha}{2}},$$

which follows from (1.16). □

To ascertain the applicability of Corollaries 11 and 12, some typical parameter values for $km=(\frac{\rho g S_0}{2\gamma})$ and for $ck^{\alpha/2}=\frac{\hat{A}}{\gamma}\left(\frac{\rho g}{2\gamma}\right)^{\alpha/2}$ are given in Table 2. It is possible to see from the last line in Tables 1 and 2 that N may be large even when $km<1$. Corollary 12 and Theorem 9 now imply Theorem (B) stated in the Introduction.

Proof The proof of Theorem 10 is contained in Lemmas 13 and 14 which follow.

Lemma 13 *Suppose that* f *satisfies Hypothesis HI* and* $\overline{K}m>1$, *then* $N>N_\infty(1-2/\bar{K}m)$, *where* $N_\infty=B_\infty/A_\infty$.

Proof From (2.14) and (2.26) it follows that

$$\frac{m}{2}\leqslant\max_{g\in[0,1]}u(A,g)\max_{g\in[0,1]}u_g(A,g)\int_0^1\frac{g}{\sqrt{1-g^2}}\,dg. \tag{3.13}$$

https://doi.org/10.1017/S0956792501004478 Published online by Cambridge University Press

Since $\max_{g\in[0,1]} u(A,g) = u(A,1) = B$ and

$$\max_{g\in[0,1]} u_g(A,g) = \left(\min_{u\in[A,B]} g_u(A,u)\right)^{-1} = \left(\frac{f(A)}{A} - f'(B)\right)^{-1},$$

we obtain from (3.13) that

$$\frac{f(A)}{A} - f'(B) \leqslant \frac{2B}{m}. \tag{3.14}$$

Since according to Claim 7, $\frac{\partial}{\partial\xi}(f(\xi)/\xi) < 0$ for $\xi \in (0, A_\infty)$, we obtain using (3.14) that for $0 < A < A_\infty$ and $0 < B < B_\infty$,

$$\frac{f(A)}{A} - f'(B) \leqslant \frac{2B}{m} < \frac{2B_\infty}{m} \quad \text{and} \quad \frac{f(A)}{A} > \frac{f(A_\infty)}{A_\infty} = f'(B_\infty).$$

Hence,

$$f'(B_\infty) - f'(B) < \frac{2B_\infty}{m}.$$

Noting that by **Hypothesis HI*** and by the hypotheses of the theorem, $f'' \geqslant \bar{K} > 0$, for $0 < \xi < B_\infty$, it follows that

$$B_\infty - B < \frac{2B_\infty}{\bar{K}\, m}.$$

Therefore,

$$N > \frac{B}{A_\infty} = N_\infty\left(\frac{B}{B_\infty}\right) > N_\infty\left(1 - \frac{2}{\bar{K}\, m}\right),$$

proving the claim of the lemma. □

Lemma 14 (i) *If* $f(\xi_{\min}) < 0$, *then* $N_\infty > \frac{1}{\xi_{\min}}$ *or more explicitely*

$$N_\infty > \left(\frac{K_1}{\alpha c}\right)^{\frac{1}{2+\alpha}}. \tag{3.15}$$

and (ii) *if* $f(\xi_{\min}) > 0$, $K_2 < 2K_1$, *and* $c < \left(\frac{2}{K_2}\right)^{\frac{\alpha}{2}}(1+b)^{\frac{2+\alpha}{2}}$ *then*

$$N_\infty > \left(\frac{K_1 - \frac{1}{2}K_2}{(1+\alpha)c}\right)^{\frac{1}{2+\alpha}}. \tag{3.16}$$

Proof Throughout the proof of the lemma, b, α, c and m will be taken to be fixed, though in a number of instances either b or c will be set equal to zero. We note that for a given function $\bar{f}$, B_∞ can be considered a function of b, α, and c. In particular, we define $B_\infty^{c=0} = B_\infty(b, \alpha, 0)$, i.e. $B_\infty^{c=0}$ is the value assumed by B_∞ when in equation (2.23) which defines B_∞, c is set equal to zero in the form (3.6) assumed for f (in other words, $f(\xi)$ is replaced by $f(\xi) - c\xi^{-\alpha}$). It follows from the definition of $B_\infty^{c=0}$ and (3.6) that

$$f'(B_\infty^{c=0}) - \frac{f(B_\infty^{c=0}) + 1}{B_\infty^{c=0}} \leqslant 0. \tag{3.17}$$

Since $f + 1$ is convex and $(B_\infty, f(B_\infty))$ lies on the unique tangent to $f + 1$ which passes through the origin, (3.17) and our scaling assumptions imply that

$$1 = B_\infty \geqslant B_\infty^{c=0}. \tag{3.18}$$

https://doi.org/10.1017/S0956792501004478 Published online by Cambridge University Press

(The scaling, according to which $B_\infty = 1$ is based on the given fixed values of the parameters.) Let us now consider the curve $y = f(\xi)$ for $\xi > 0$. It is a convex curve with a unique minimum which occurs at $\xi_{\min}$. The conditions of the lemma imply that $\xi_{\min} < \left(\frac{\alpha c}{K_1}\right)^{\frac{1}{2+\alpha}}$. Suppose condition (i) holds, then $f(\xi_{\min}) \leqslant 0$. By the definition of A_∞ and the positivity of $f'(B_\infty)$, it follows that $A_\infty < \xi_{\min}$, and hence

$$A_\infty < \left(\frac{\alpha c}{K_1}\right)^{\frac{1}{2+\alpha}}. \tag{3.19}$$

Combining the results of (3.19) and (3.19) yields the inequality (3.15) and completes part (i) of the lemma.

Let us now suppose that $f(\xi) > 0$ for all $\xi > 0$. This will be ensured if condition (ii) in the statement of the lemma holds. Since $f(\xi)$ is convex, there will exist a unique tangent to the curve $y = f(\xi)$ which passes through the origin. Let us denote the point of tangency by $(\bar{A}, f(\bar{A}))$. It is easy to verify under these circumstances that

Claim 15 $\left(\frac{f(\xi)}{\xi}\right)' < 0$ for $\xi \in (0, \bar{A})$, and $\left(\frac{f(\bar{A})}{\bar{A}}\right)' = 0$.

Let us now define $f^{c=0}(\xi) = f(\xi) - c\xi^{-\alpha}$, i.e. $f(\xi)$ is as in (1.15) but with c set to zero. Since clearly $0 < f^{c=0}(\xi) + 1 < f(\xi) + 1$ for all $\xi > 0$, the tangent to $f^{c=0}(\xi) + 1$ which passes through the origin must lie below the tangent to $f(\xi) + 1$ which passes through the origin. Therefore,

$$\frac{f^{c=0}(B_\infty^{c=0}) + 1}{B_\infty^{c=0}} \leqslant \frac{f(B_\infty) + 1}{B_\infty}. \tag{3.20}$$

Let us now consider the equation

$$\frac{f(\xi)}{\xi} = \frac{f^{c=0}(B_\infty^{c=0}) + 1}{B_\infty^{c=0}}, \quad \xi > 0. \tag{3.21}$$

It can be checked by direct substitution that if condition *ii*) in the statement of the lemma holds, then

$$c < (1 + b)(B_\infty^{c=0})^\alpha < (B_\infty^{c=0})^\alpha. \tag{3.22}$$

Therefore

$$\frac{f^{c=0}(B_\infty^{c=0}) + 1}{B_\infty^{c=0}} > \frac{f(B_\infty^{c=0})}{B_\infty^{c=0}}.$$

Thus, in particular

$$\frac{f^{c=0}(B_\infty^{c=0}) + 1}{B_\infty^{c=0}} > \frac{f(\bar{A})}{\bar{A}},$$

which, in conjunction with the assumed behavior of $f(\xi)$ as $\xi \to 0$, guarantees that a solution to (3.21) exists. Let us now define A_1 to be the smallest positive root of (3.21). By Claim 15, we have that $A_1 < \bar{A}$. By (2.23) and (3.20), it follows that

$$\frac{f(A_1)}{A_1} \leqslant \frac{f(A_\infty)}{A_\infty},$$

thus invoking Claim 15,

$$A_\infty \leqslant A_1. \tag{3.23}$$

https://doi.org/10.1017/S0956792501004478 Published online by Cambridge University Press

Let us now define $f^{b=0}(\xi) = f(\xi) - b$, i.e. $f^{b=0}(\xi)$ is the same as $f(\xi)$ except that b has been set equal to 0, and let us consider the equation

$$\frac{f^{b=0}(\xi)}{\xi} = \frac{f^{c=0}(B_\infty^{c=0}) + 1}{B_\infty^{c=0}}, \quad \xi > 0. \tag{3.24}$$

By (3.22)

$$\frac{f^{c=0}(B_\infty^{c=0}) + 1}{B_\infty^{c=0}} > \frac{f^{b=0}(B_\infty^{c=0})}{B_\infty^{c=0}}, \tag{3.25}$$

and hence a solution to (3.24) exists. We denote the smallest positive solution to (3.24) by A_2. Let us denote by $\bar{A}_2$ the value at which $f^{b=0}(\xi)/\xi$ attains its minimum. It follows from (3.24), (3.25) and Claim 15 (formulated in terms of $f^{b=0}$) that $A_2 \leqslant \bar{A}_2$. From (3.21) and (3.24), and by noting that $f^{b=0}(\xi) \geqslant f(\xi)$ for all $\xi > 0$,

$$\frac{f(A_1)}{A_1} = \frac{f^{b=0}(A_2)}{A_2} \geqslant \frac{f(A_2)}{A_2}.$$

Since $A_1 \leqslant \bar{A}$, by Claim 15 and (3.23)

$$A_\infty \leqslant A_1 \leqslant A_2 \leqslant \bar{A}_2. \tag{3.26}$$

A straightforward calculation based on Hypothesis HI* yields that that

$$\bar{A}_2 < \left(\frac{(1+\alpha)c}{K_1 - \frac{1}{2}K_2} \right)^{\frac{1}{2+\alpha}}. \tag{3.27}$$

Combining (3.18), (3.26) and (3.27), the estimate (3.16) follows. □

□

4 Conclusions

The inclusion of a disjoining pressure in the expression for the free energy of a droplet is by its nature problematic in that it reflects an attempt to incorporate mesoscopic effects in a continuum model. Surface energies are at once taken into account by both singular contributions – which were really designed for planar or mildly sloped surfaces, and by the regular or classical surface energy contributions. One must be pleased by the robustness of the physical predictions given the relative carelessness of the physical modelling. Hopefully, our results shall contribute to the development of dynamic theories of droplet and thin film motion with compact support.

Acknowledgements

The basis of this work appeared in 1994 as part of the M.Sc. thesis of E. Minkov (Technion-IIT, Israel), entitled, *Effects of disjoining pressure in contact angle problems* (in Hebrew). The authors would like to thank L. Giacomelli for reading and commenting on an earlier version of this manuscript, and an anonymous referee for many helpful questions and comments. The authors would further like to thank J. W. Cahn, A. Marmur, A. Oron and D. Shechtman for their comments with regard to the limits of microscopy. One of

the authors (A. N.-C.) would like to acknowledge the support of *Fund for the Promotion of Research at the Technion.*

References

[1] Bernis, F. & Friedman, A. (1990) Higher order nonlinear degenerate parabolic equations. *J. Diff. Eqn.* **83**, 179–206.
[2] Bertozzi, A. L. & Pugh, M. (1994) The lubrication approximation for thin viscous films: the moving contact line with a 'porous media' cut-off of van der Waals interactions. *Nonlinearity*, **7**, 1535–1564.
[3] Cesari, L. (1983) *Optimization- Theory and Applications.* Springer-Verlag.
[4] Derjaguin, B. V., Churaev, N. V. & Muller, V. M. (1987) *Surface Forces.* Consultants Bureau, New York.
[5] Dussan V, E. B., Ramé, E. & Garoff, S. (1991) On identifying the appropriate boundary conditions at a moving contact line: an experimental investigation. *J. Fluid Mech.* **230**, 97–116.
[6] Edington, J. W. (1991) *Practical Electron Microscopy in Materials Science.* MacMillan.
[7] Finn, R. (1986) *Equilibrium Capillary Surfaces.* Springer-Verlag.
[8] Giacomelli, L. & Otto, F. (2000) Variational formulation for the lubrication approximation of the Hele-Shaw flow. Preprint.
[9] Grün, G. On the numerical simulation of wetting phenomena. *Proc. 15th GAMM Workshop 'Numerical methods for composite materials'.* Vieweg-Verlag, Braunschweig.
[10] Herminghaus, S., Jacobs, K., Mecke, K., Bischof, J., Fery, A., Ibn-Elhaj, M. & Schlagowski, S. (1998) Spinodal dewetting in liquid crystal and liquid metal films. *Science*, **282**, 916–919.
[11] Jameel, A. T. & Sharma, A. (1994) Morphological phase separation in thin liquid films. *J. Colloid Interface Sci.* **164**, 416–427.
[12] Laugesen, R. S. & Pugh, M. C (2000) Energy levels of steady states for thin film type equations. Preprint.
[13] Laugesen, R. S. & Pugh, M. C. (2000) Properties of steady states for thin film equations. *Euro. J. Appl. Math.* **11**, 293–351.
[14] Minkov, E. (1994) *Effects of disjoining pressure in contact angle problem.* MSc Thesis, Technion-IIT, Israel.
[15] Mitlin, V. S. (1993) Dewetting of solid surface: analogy with spinodal decomposition. *J. Colloid Interface Sci.* **156**, 491–497.
[16] Mitlin, V. S. & Petviashvili, N. V. (1994) Nonlinear dynamics of dewetting: kinetically stable structures. *Phys. Lett. A* **192**, 323–326.
[17] Marmur, A. (1996) Equilibrium contact angels: theory and measurement, *Colloids and Surfaces*, **116**, 55–61.
[18] Novick-Cohen, A. (1992) On a minimization problem arising in wetting, *SIAM Appl. Math.* **52**, 593–613.
[19] Novick-Cohen, A. (1993) A singular minimization problem for droplet profiles, *Euro. J. Appl. Math.* **4**, 399–418.
[20] Oron, A. (2000) Three-dimensional nonlinear dynamics of thin liquid films. *Phys. Rev. Lett.* **85**, 2108–2111.
[21] Oron, A. & Bankoff, S. G. (1999) Dewetting of a heated surface by an evaporating liquid film under conjoining/disjoining pressures. *J. Colloid Interface Sci.* **218**, 152–166.
[22] Oron, A., Davis, S. H. & Bankoff.S. G. (1997) Long-scale evolution of thin liquid films, *Rev. Mod. Phys.* **69**, 931–980.
[23] Otto, F. (1998) Lubrication approximation with prescribed nonzero contact angle: an existence result, *Comm. PDEs,* **23**, 2077–2161.
[24] Paulsen, F. G., Pan, R., Bousfield, D. W. & Thompson, E. V. (1996) The dynamics of

bubble/particle attachment and the application of two disjoining film rupture models to flotation. *J. Colloid Interface Sci.* **178**, 400–410.

[25] Teletzke, G. F., Davis, H. T. & Scriven, L. E. (1988) Wetting hydrodynamics. *Rev. Phys. Appl.* **23**, 1473–1484.

[26] Von Weizsacker, C. C. (1965) Existence of optimal programs of accumulation for an infinite horizon, *Rev. Econ. Stud.* **32**, 85–104.

[27] Williams, M. B. & Davis, S. H. (1982) Nonlinear theory of film rupture. *J. Colloid Interface Sci.* **90**, 220–228.